Surface morphology and ionization potentials of polar semiconductors: The case of GaAs

C. Sgiarovello
Institut Romand de Recherche Numérique en Physique des Materiaux (IRRMA), CH–1015 Lausanne, Switzerland

N. Binggeli
International Center for Theoretical Physics (ICTP) and INFM DEMOCRITOS National Simulation Center, Strada Costiera 11, I-34014 Trieste, Italy

A. Baldereschi
Institut Romand de Recherche Numérique en Physique des Matériaux (IRRMA) and Institute of Theoretical Physics, EPFL, CH-1015 Lausanne, Switzerland
and Dipartimento di Fisica Teorica and INFM, Universitá di Trieste, I-34014 Trieste, Italy
(Received 1 September 2003; published 27 January 2004)

Using an *ab initio* pseudopotential approach, we have studied the ionization potential of several surfaces of GaAs, with different orientation, reconstruction, and stoichiometry. In particular, we have examined the As-rich (100) c-(4×4), $(2\times4)2\beta$, and $(2\times4)\beta$ surfaces, the Ga-rich (100) $(4\times2)2\beta$ and $(4\times2)\zeta$ surfaces, as well as the (110) surface. The calculated variations of the ionization potential with surface morphology are as large as 0.7 eV. The largest ionization potential (5.70 eV) occurs for the As-rich $(2\times4)\beta$ surface, and the smallest (5.00 eV) for the Ga-rich $(4\times2)2\beta$ one. The results are compared with available experimental data, and are explained in terms of a model based on a superposition of neutral bulk charge-density units, carrying neither dipole nor quadrupole, and charge transfers between the units dictated by the electron counting rule.

DOI: 10.1103/PhysRevB.69.035320 PACS number(s): 73.30.+y, 79.60.Bm, 68.35.Md

I. INTRODUCTION

The ionization potential (IP) is a crucial parameter in a wide range of phenomena including photoemission, thermoionic emission, adsorption, and catalysis.[1–3] It is known to depend on surface-specific structural and chemical features. Such a dependence is exploited, e.g., in the fabrication of GaAs photocathodes using cesiated surfaces.[4] It is also a potentially sensitive tool for surface characterization, e.g., *in situ* monitoring of surface growth processes during molecular-beam epitaxy MBE.[5–7]

For clean GaAs surfaces, experimental studies[8–11] indicate substantial variations [up to 0.8 eV (Ref. 9)] of the work function (WF) and IP with the surface atomic geometry. In particular, the GaAs (100) IP and WF show large (0.4–0.6 eV), nonmonotonous changes when the As-richest (100) c-(4×4) structure is heated—driving As out from the surface—and undergoes a series of reconstructions producing sequentially (2×4) As-rich phases, some partially ordered (3×1), (1×6), and (2×6) structures, and finally a Ga-rich (4×2) phase. The effects of surface reconstruction and/or stoichiometry on the IP have not been extensively investigated. Surface stoichiometry, reconstruction, and crystallographic orientation are not independent variables for describing clean III-V semiconductor surfaces. In fact, the known surface reconstructions of most III-V semiconductors, and in particular those of GaAs, verify the electron counting rule,[12] which stipulates that all anion dangling bonds should be full and all cation dangling bonds empty to make the surface nonmetallic and stable. This interplay between surface stoichiometry, reconstruction, and crystallographic orientation makes the dependence of the IP on surface geometry a rather complex problem, which has remained largely unexplored theoretically. To our knowledge, *ab initio* calculations of the GaAs IP have been performed only for the (110) surface[13–15] and for the (2×4) reconstruction of the (100) surface.[16] Furthermore, surface-dipole models have been proposed to explain the IP variation among (100) reconstructions having the same type of adatom-dimer surface structural units.[8]

In this work, we examine several different surfaces of GaAs(100), as well as the GaAs(110) surface, by means of *ab initio* calculations, and study the dependence of the IP on surface orientation, stoichiometry, and reconstruction. We find large variations of the IP with surface morphology, consistent with available experimental data. The calculated and observed IP trends are explained by a surface-dipole model that takes into account the charge transfers between bulk-building units which are dictated by the electron counting rule. This model generalizes previous results[8] by allowing comparison between surfaces having different orientations and, for a given polar orientation, different reconstructions.

II. METHOD

Our study is performed within density-functional theory (DFT) using the local-density approximation (LDA) with the exchange-correlation potential of Ceperley and Alder.[17] We employ Troullier-Martins[18] pseudopotentials in the fully nonlocal Kleinman-Bylander form[19] and a plane-wave basis set. The surfaces are modeled using a slab geometry in supercells.[20] For the (110) and the (100) c-(4×4) surfaces, we use 15-monolayer-thick GaAs slabs that are terminated by two equivalent surfaces. For the (100) (2×4) and (4×2) surfaces, we employ GaAs slabs containing 12–15

 ©2004 The American Physical Society

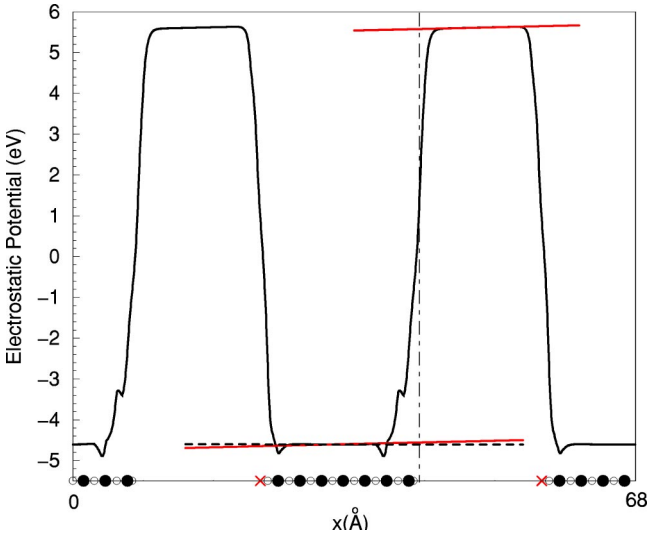

FIG. 1. Macroscopic average of the electrostatic potential in the periodic slab geometry used to model the Ga-rich GaAs (100) $(4\times2)2\beta$ surface. The GaAs$(4\times2)2\beta$ surface is at the right-hand side of each slab while, on the left-hand side, the slabs are terminated by a bulk-truncated H-passivated surface. The positions of the atomic planes in the slabs are indicated at the bottom of the figure. Ga atoms are indicated by small empty circles, As atoms by large filled circles, while the small crosses represent virtual hydrogen atoms. The straight line is a linear fit of the electrostatic potential in the vacuum region (its replica is also shown in the bulk part). The dashed line is a linear fit to the potential in the bulk region. The surface-potential step ΔV is evaluated on the vertical dot-dashed line, placed at one-half of a bulk interlayer distance ($\sim$0.7 Å) from the outermost atomic layer of the slab.

atomic layers, and we passivate the Ga layer at one termination with virtual hydrogen atoms with fractional charge $Z=1.25$. We note that the passivated slabs correspond to supercells whose lateral section corresponds to the actual unit cell of the reconstructed surface, while slabs with two equivalent surfaces would require much larger sections, because of the 90° rotoreflection that relates the two surfaces. The vacuum regions separating contiguous slabs are $\sim$14 Å thick in all cases.

As in previous work,[21,22] we evaluate the IP as the sum of two contributions: $E_I=\Delta V-E_{VBM}$, where E_{VBM} is the position of the valence-band maximum measured with respect to the average electrostatic potential in bulk GaAs and ΔV is the electrostatic potential step at the surface. Only ΔV depends on the structural and chemical details of the surfaces. E_{VBM} is obtained from standard bulk band-structure calculations, while ΔV is derived from the macroscopic average of the electrostatic potential obtained from the supercell calculations.[22]

We note that, in the case of (100) slabs with two inequivalent surfaces, a constant electric field can be present in the slabs and/or in the vacuum regions separating the periodically repeated slabs. This can be seen in Fig. 1, where we display the calculated macroscopic average of the electrostatic potential for the GaAs(100) $(4\times2)2\beta$ surface. The electric field is strongly screened within the GaAs slabs (the calculated value[23] of the dielectric constant of GaAs is $\epsilon_\infty^{\mathrm{GaAs}}=12.4$). The presence of electric fields in the supercell complicates somewhat the determination of the surface-potential step, as one needs to know the position of the intrinsic surface dipole to measure precisely ΔV.[24] From previous work,[22,25] this position is known to be roughly at half-an-interlayer distance outside the outermost atomic layer ($\sim$0.7 Å in our case), and this is the position we systematically use in the present work to calculate ΔV (see Fig. 1). We note, however, that the electric fields that are present in our systems are rather small, so that changing this position by ±1.4 Å has a negligible influence (less than 30-meV change) on the calculated IP values.

The bulk and supercell calculations are carried out using a 20-Ry kinetic energy cutoff for the plane-wave expansion of the electronic wave functions. The integrations in reciprocal space are preformed using a Monkhorst-Pack[26] grid of dimension (4,4,2) for the c-(4×4) reconstruction and (4,8,2) in all other cases. For the structural optimization, we allow the four outermost atomic layers of the GaAs surfaces to fully relax. At the passivated surface, we let the virtual hydrogen and the outermost-Ga layer to fully relax. A steepest-descent approach is used for the atomic relaxation, and the process is stopped when the forces on the atoms are smaller than 0.005 Ry/a.u. With the above values of the computational parameters, including slab and vacuum thicknesses, we estimate that the calculated values of the IP are converged to within 50 meV.

Our LDA values of the IP should be corrected to include (i) spin-orbit, (ii) many-body, and (iii) semicore-orbital effects. The spin-orbit splitting Δ_{SO} of the GaAs valence-band edge, neglected in our scalar-relativistic calculations, increases E_{VBM} by $\Delta_{SO}/3$. Using the experimental value of Δ_{SO} (0.34 eV),[27] the spin-orbit correction to the LDA IP value is thus -0.11 eV. For the many-body correction, we use the result of the GW calculations by Needs *et al.*,[28] who obtained a quasiparticle correction of -0.36 eV to the LDA GaAs valence-band-edge energy. This increases the IP by $+0.36$ eV. Finally, the Ga-3d orbitals, which are treated as frozen-core states in our pseudopotential calculations, produce a rigid $+0.1$-eV shift of the GaAs bulk-valence-band edge when treated as valence orbitals in GaAs-based semiconductor heterojunctions and metal/semiconductor junctions.[29] Assuming that the same shift applies to GaAs surfaces, semicore-orbital effects yield an additional correction of -0.1 eV to the IP. Summing up, the total correction due to spin-orbit, many-body, and semicore-orbital effects on the LDA IP value amounts to $\Delta=+0.15$ eV.

The overall uncertainty on the LDA-corrected absolute values of the IP is estimated as 0.1 eV. As usual, however, using LDA/DFT calculations, the uncertainty on the relative values of the IP between different GaAs surfaces is expected to be smaller, i.e., of the order of our numerical accuracy of $\sim$50 meV.

III. *Ab initio* RESULTS

A. Formation energies

The atomic geometries of the reconstructed GaAs (100) surfaces considered in this work are illustrated in Fig. 2. We

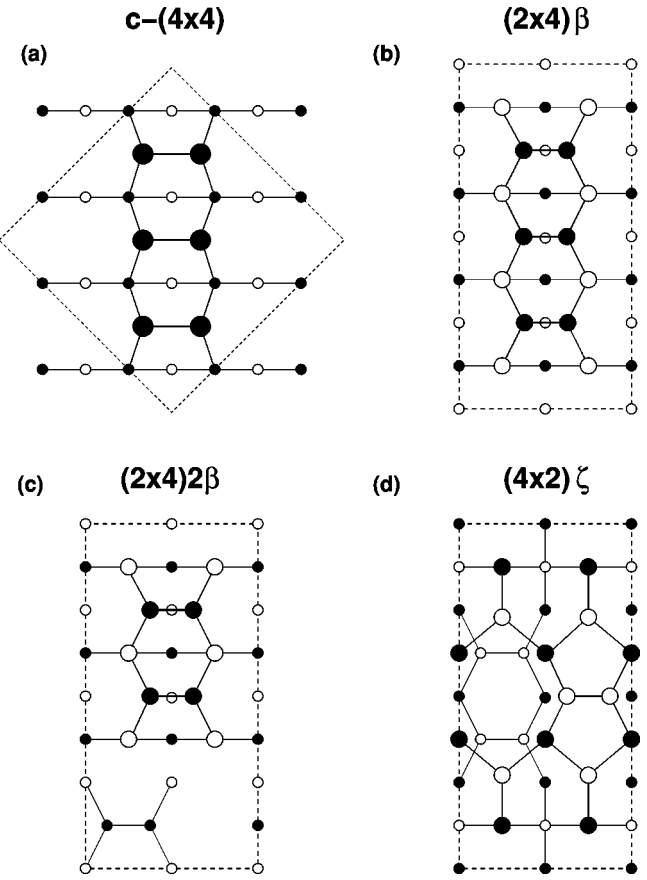

FIG. 2. Top views of the GaAs (100) c-(4×4) (a), $(2\times4)\beta$ (b), $(2\times4)2\beta$ (c), and $(2\times4)\zeta$ (d) reconstructed surfaces. The surface unit cell is indicated by the dashed lines. Large (small) filled circles represent top- (third-) layer As atoms, while large (small) empty circles correspond to second- (fourth-) layer Ga atoms.

consider the As-rich c-(4×4) three-dimer structure,[30] the As-terminated $(2\times4)\beta$ and $(2\times4)2\beta$ geometries,[31,32] the Ga-rich $(4\times2)\zeta$ structure,[33] and the Ga-terminated $(4\times2)2\beta$ configuration[32] which is obtained by interchanging Ga and As atoms in the As-terminated $(2\times4)2\beta$ structure.

The three-dimer structure, in Fig. 2(a), is the commonly accepted model of the c-(4×4) atomic geometry; this is also the As-richest structure examined in our work. This structure corresponds to an As-terminated surface with on top 3/4 of a dimerized monolayer of As; the top layer is organized in rows of three-dimer structures separated by half of a structure length with respect to each other. The accepted geometry of the (2×4) reconstruction, which is observed in MBE under As-rich condition, is the 2β configuration displayed in Fig. 2(c). An earlier competitive model for this reconstruction is the β configuration shown in Fig. 2(b). The β configuration corresponds to a dimerized As-terminated surface from which one dimer out of four has been removed. The 2β structure can be obtained from the β structure by removing two As and two Ga atoms from the outermost As and Ga layer in each (2×4) unit cell, and letting the As atoms with broken bonds from the layer underneath dimerize. The ζ configuration, in Fig. 2(d), is a complex structure which has been recently proposed by Lee *et al.*[33] as the stable geometry

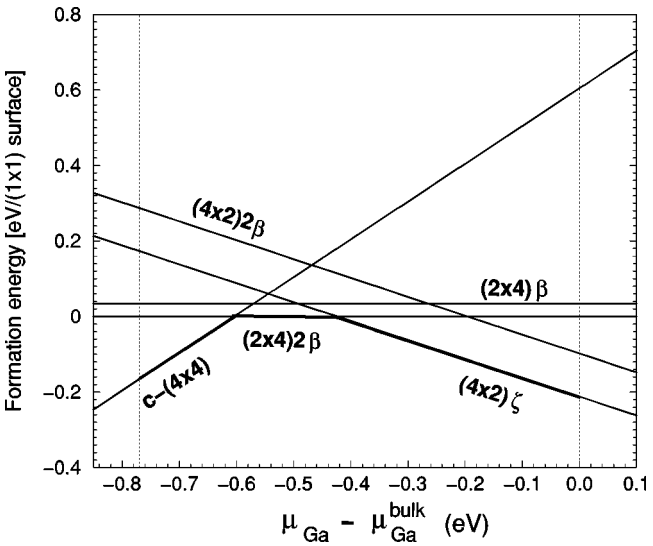

FIG. 3. Calculated formation energies [in units of eV per (1×1) surface unit cell] of the various GaAs(100) surfaces studied in the present work. The zero of energy is set at the formation energy of the $(2\times4)2\beta$ structure. The vertical, dotted lines indicate the allowed range for the Ga chemical potential ($-\Delta H_f \leqslant \mu_{\mathrm{Ga}} - \mu_{\mathrm{Ga}}^{bulk} \leqslant 0$, with $-\Delta H_f = -0.77$ eV).

of the (4×2) reconstruction observed under Ga-rich conditions. An earlier model for this reconstruction is the Ga-terminated 2β structure.

The above structures are those with the lowest energy among the structures that have been proposed for the reconstructions considered here. In Fig. 3, we show their formation energies as a function of the Ga chemical potential μ_{Ga}. The convergence on the relative values of the surface formation energies is estimated to be 10 meV per (1×1) surface unit cell. The formation energies are calculated relative to the formation energy of the $(2\times4)2\beta$ structure and are displayed over the thermodynamically allowed range of μ_{Ga}, given by $-\Delta H_f \leqslant \mu_{\mathrm{Ga}} - \mu_{\mathrm{Ga}}^{bulk} \leqslant 0$, where ΔH_f is the heat of formation of GaAs and μ_{Ga}^{bulk} is the chemical potential of bulk orthorhombic Ga metal. We find $\Delta H_f = 0.77$ eV, in good agreement with the experimental value of 0.85 eV (Ref. 34) and with the results of previous calculations.[16,35,36]

Our results indicate that, in the limit of As-rich conditions, the c-(4×4) structure is the most stable configuration at zero temperature. At larger values of μ_{Ga}, the $(2\times4)2\beta$ structure becomes more favorable, and at still higher values of μ_{Ga}, the $(4\times2)\zeta$ structure becomes the most stable geometry. These results are in general agreement with the results by Lee *et al.*[33] and are also consistent with previous calculations for the As-rich structures.[16,32,35,36] We find, however, that the $(2\times4)\beta$ structure has a formation energy which is only $\sim$35 meV larger than that of the 2β structure. This is somewhat smaller (by $\sim$15 meV), but not inconsistent with the results by Lee *et al.*,[33] who quoted a numerical uncertainty of 10 meV in their calculations.

The results in Fig. 3 are consistent with the experimental reconstruction trends, but should be considered with some caution when discussing the atomic structures of the experimentally observed reconstructions. Indeed, at experimental

TABLE I. Calculated and experimental values of the IP (in eV) for different GaAs (100) reconstructions and for the GaAs (110) surface. LDA and LDA-corrected values are given, the correction being a rigid shift of +0.15 eV, to account for many-body, spin-orbit, and semicore-orbital effects. The experimental values are from Refs. 37(a), 5(b), 38(c), 39(d), and 40(e).

	(100)					(110)
	c-(4×4)	(2×4)β-type		(4×2)Ga-rich		
	Trimer	β	2β	ζ	2β	
LDA	5.09	5.55	5.11	5.04	4.85	5.10
LDA-corr.	5.24	5.70	5.26	5.19	5.00	5.25
Expt.	5.29[a]	5.5[b]				5.40[c], 5.56[d], 5.15[e]

conditions, the calculated $T=0$ formation energies may not be appropriate to discriminate between structures that are rather close in energy, since kinetic effects may come into play. This concerns, for example, the (2×4)β and (4×2)2β structures, which should be considered as energetically competitive structures under As-rich and Ga-rich conditions, respectively.

B. Ionization potentials

The calculated IP values for the (110) surface and several (100) reconstructions are given in Table I. We report the LDA values, as well as the results corrected for many-body, spin-orbit, and semicore-orbital effects. The correction amounts to a shift of +0.15 eV, and should not affect IP trends with surface morphology. The calculated IP values show a significant variation (0.7 eV) with surface atomic geometry. The largest IP value (5.70 eV) is obtained for the As-terminated (2×4)β structure, the lowest value (5.0 eV) is found for the Ga-rich (4×2)2β structure, and the other structures have IP values of about 5.2 eV.

Our LDA value for the IP of the (110) surface is in good agreement with the LDA value of 5.07 eV calculated by Adamowicz and Zbroszczyk,[13] and also in fair agreement with the values of 5.02 eV and 4.94 eV obtained in earlier calculations.[14,15] Schmidt and Bechstedt[16] reported LDA IP values of 5.5 eV and 5.43 eV for the As-rich (2×4)β and 2β structures, respectively. The value they found for the β structure agrees well with ours, but that of the 2β structure is ~0.3 eV larger than ours. This difference is likely due to the very thin slab (eight atomic layers) used by these authors; indeed we find that no less than 12 layers are needed to obtain converged IP values.

The LDA-corrected values in Table I compare well with available experimental data, both for the (100) and (110) surfaces. A value of 5.29 eV has been reported from photoemission-yield spectroscopy for the IP of the (100) c-(4×4) surface,[37] in very good agreement with our value of 5.24 eV. For the As-rich (100) (2×4)β-type phase obtained by MBE, the measured value is 5.5 eV,[5] which is intermediate between our calculated values for the (2×4)2β and β structures. The close value of 5.35 eV has been reported for the IP of (100) (2×4)c-(2×8) MBE-grown surface.[37] For the (110) surface, the experimental values range from 5.15 to 5.56 eV,[38–40] to be compared with our calculated value of 5.25 eV.

Work function changes induced by sequential annealing of GaAs (100) As-rich c-(4×4) surfaces have been measured in Refs. 8 and 9, by contact potential difference, as a function of annealing temperature. These changes in WF are expected to follow closely the IP changes, as the Fermi energy has been measured to remain confined within a narrow energy window (width ~0.1 eV) near midgap at such surfaces.[8] The starting c-(4×4) surfaces were either *in situ*-fabricated[9] or As-decapped[8,9] MBE-grown surfaces. Although some of the measured variations are smaller for As-decapped than for *as-grown* MBE surfaces, the trends with annealing temperature are similar. As the annealing temperature increases and the As desorbs from the surface,[8] the WF shows first a large increase (0.2 eV for decapped and 0.4 eV for *in situ* fabricated surfaces) that occurs when the surface reconstructs from the As-richest c-(4×4) to an As-rich (2×4)c-(2×8) type of geometry, at about 400 °C. This is followed, from 450 °C to 550 °C, by a drastic decrease of the WF's [a 0.2-eV WF lowering with respect to the starting c-(4×4) geometry] when the surface changes from the (2×4)c-(2×8) to a Ga-rich (4×2)c-(8×2) structure. Finally, the WF value increases again towards the initial value when the temperature is raised up to 700 °C, the surface remaining in the (4×2)c-(8×2) configuration. An overall variation of 0.6 eV (0.4 eV) is thus observed when annealing the MBE-grown (decapped) c-(4×4) surfaces.

The smaller initial increase in the WF measured for the As-decapped samples, responsible for the smaller overall WF variation observed with such samples, was attributed[9] to the less well-ordered initial c-(4×4) and resulting (2×4)c-(2×8) structures obtained by decapping than by MBE growth. The authors of Ref. 9 in fact also directly fabricated *in situ* As-rich (2×4)c-(2×8) surfaces that showed even sharper low-energy electron-diffraction patterns than the ones obtained by annealing MBE-grown c-(4×4) surfaces. They obtained in this way overall WF variations with surface reconstruction as large as ~0.8 eV.

The above WF changes and trends are generally consistent with the calculated IP variations with Ga coverage shown in Fig. 4. The calculations also suggest that the atomic structure of the As-rich (2×4) surfaces fabricated by MBE (Ref. 9) is likely the β structure, and not the 2β structure, in spite of its lower $T=0$ formation energy. Similarly, the β structure is likely the one which is responsible for the large WF increase observed in the (2×4)c-(2×8) reconstruction

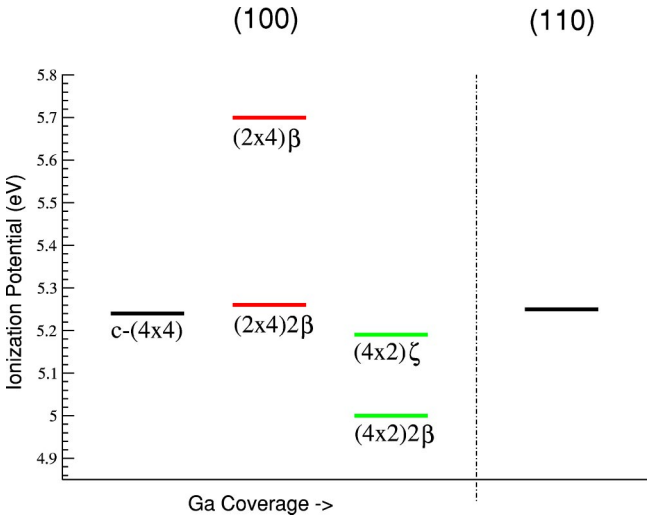

FIG. 4. Corrected LDA values of the IP for various GaAs (100) reconstructions (left) and the (110) (right) surface obtained in this work. The IP's of the (100) surfaces are reported as a function of increasing Ga coverage of the surface.

FIG. 5. Schematic representation of the tetrahedral Ga and As bulk-building blocks used to construct the reference charge in our model.

regime when annealing c-(4×4) surfaces.[8,9] Finally, our results indicate that the Ga-rich $(4\times2)2\beta$ structure is likely the one responsible for the large WF decrease observed in the $(4\times2)c$-(8×2) reconstruction regime from 450 °C to 550 °C.[8,9]

IV. SURFACE-DIPOLE MODEL

The IP values obtained in the *ab initio* calculations and illustrated in Fig. 4 suggest the possibility of a simpler description to predict the IP trends with surface atomic geometry. In particular, we notice that the IP's of the (110) and (100) c-(4×4) surfaces are practically identical, while that of the As-rich $(2\times4)\beta$ [Ga-rich $(4\times2)2\beta$] surface is much larger [smaller] than these values. We propose a dipole model to understand these features and qualitatively predict the IP changes when the surface atomic geometry is modified.

The model describes the surface charge in terms of bulk-building blocks and electron transfers dictated by the electron counting rule (ECR). It is a generalization of the approach proposed by Chen *et al.*, who examined the GaAs(100) As-terminated $(2\times4)\beta$, Ga-terminated $(4\times2)\beta$, and c-(4×4) surfaces.[8] We note that the latter cases involve only adatom-dimer reconstructions, and the correct relative trend of the surface dipoles is obtained by simply considering the charge transfers, derived from the ECR, between atoms in the final, equilibrium reconstructed surface geometries.[8] However, this scheme does not apply to more complex reconstructions, with larger structural rearrangements, and predicts, for example, the wrong sign for the dipole change from the $(4\times2)2\beta$ surface to the c-(4×4) surface. By explicitly introducing an appropriate reference system for the various surfaces, we are able to describe the IP trends of a wider class of surface atomic geometries, including surfaces with different crystallographic orientations and, for a given orientation, reconstructions with very different structural patterns.

The model is based on a reference atomic structure for each surface in which all atoms occupy positions which are as close as possible to those obtained in *ab initio* calculations and such that they have bond lengths and bond angles with

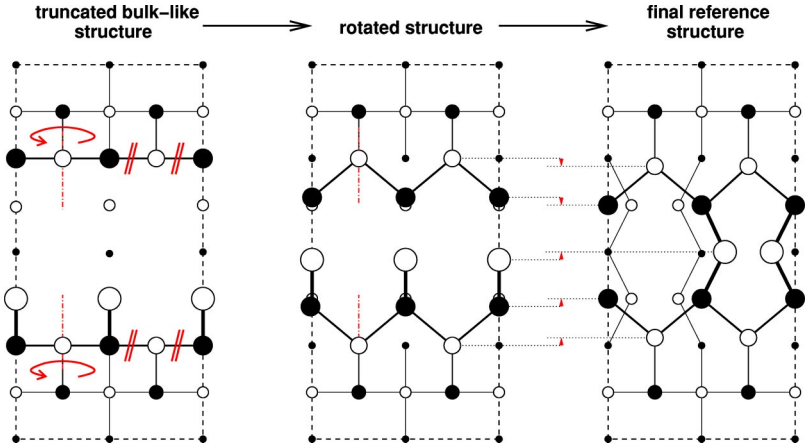

FIG. 6. Schematic representation (top view) showing how the reference structure for the GaAs(100) $(4\times2)\zeta$ reconstruction (right-hand side panel) is obtained starting from a truncated bulklike structure (left-hand side panel): first some Ga-As surface bonds are broken and GaAs bulklike fragments on top of the surface are rigidly rotated by 180° about the axis passing through the Ga-As bond that binds the fragment to the surface (indicated with the dot-dashed lines). This leads to the ''rotated'' structure shown in the central panel. In order to obtain a ''closed'' structure, in addition to the dimer formation, atoms must also be slightly shifted laterally toward the center of the cell (arrows). The symbols for the Ga and As atoms are as in Fig. 2.

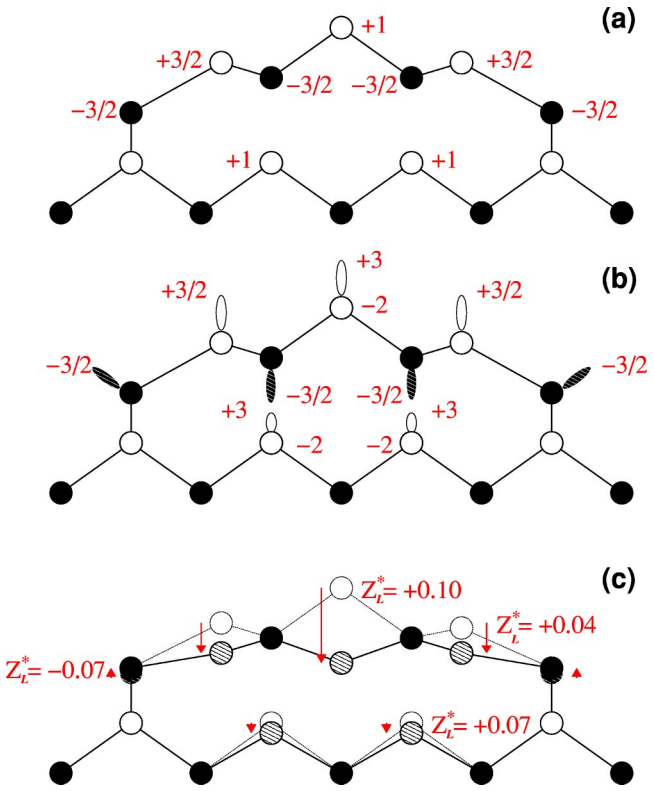

FIG. 7. Side views of the reference structure for the GaAs(100) $(4\times2)\zeta$ reconstruction illustrating the electron charge transfers considered in model 1 (a) and model 2 (b), and the ionic relaxation from the reference structure to the $(4\times2)\zeta$ structure (arrows and gray circles) (c) also considered in model 2. The calculated dynamical longitudinal charges (Z_L^*) of the surface atoms are also shown in panel (c).

their first-nearest neighbors equal to those in bulk GaAs.

The reference system is then obtained by a superposition of bulk-building blocks of charge densities centered on the sites of the reference atomic structure. This step is analogous to the construction of reference metal surfaces in terms of bulk Wigner-Seitz cells in Smoluchowski's model[41] to explain metal WF anisotropies. For semiconductors we define the reference surface as a linear superposition of frozen tetrahedral As- and Ga-sp^3-like building blocks, where the electronic charge of the neutral atom is equally distributed on the bonds, as illustrated in Fig. 5. Such entities are neutral and have neither dipole nor quadrupole, so that all GaAs surfaces obtained as a superposition of such frozen building blocks have the *same* surface dipole and therefore the same IP, independent of the surface crystallographic orientation and of the local arrangement of the building blocks at the surface.[42]

In practice, most of the GaAs surface structures can be viewed either as a bulk-truncated surface [e.g., the (110) surface] or as a bulk-truncated surface from which some cation and/or anion have been removed and/or added at selected atomic crystal sites [this is the case, e.g., of the (100) c-(4×4), $(2\times4)\beta$, and 2β surfaces]. Lateral displacements of atoms at the surface (e.g., to form dimers) are assumed here to have a negligible effect on the IP (in practice, this effect is zero only to the first order in the lateral displacement of the ions).[43] Since additions/removals of rigid As (or Ga) bulk-building blocks of charge do not affect the IP, all starting structures have the same reference IP, provided the As and Ga bulk-building blocks are kept frozen at the surface.

In the case of the $(4\times2)\zeta$ structure, the construction of the reference surface from a bulk-truncated surface is more complicated. Starting from the bulk-truncated structure with missing atoms shown on the left-hand side of Fig. 6, the ζ structure can be derived by breaking some Ga-As surface bonds and rigidly rotating the resulting GaAs bulklike fragments on top of the surface by 180° about the axis passing through the Ga-As bond that binds the fragment to the surface. This is illustrated in Fig. 6. We note that this reference structure (which has a surface dipole identical to those of the other reference structures discussed above) is not as close to the final reconstructed atomic geometry as in the other cases, since the central Ga dimer is still above the neighboring As atoms, while it should be below them [see Fig. 7(c)]. However, this model structure is a good reference, given the complexity of the ζ structure.

Electronic relaxation relative to the reference distribution is then included by populating the surface bonds according to the electron counting rule, i.e., filling dimer, covalent, and As-dangling bonds with two electrons, and removing the electrons from the Ga-dangling bonds. The resulting electron transfers among the As and Ga blocks produce surface dipoles that depend on the surface atomic geometry. As a first approximation, we model these charge transfers by point charges centered on the ions. The IP change is then obtained from the dipole generated by such point charges on the atomic planes [see Fig. 7(a) for the $(4\times2)\zeta$ structure], screened by the GaAs dielectric constant $\epsilon_\infty=12.4$.[23] The resulting IP changes obtained for the various surfaces are given in Table II (model 1). The IP change with respect to the

TABLE II. Model predictions for the IP changes (in eV) of the different (100) reconstructed surfaces relative to the (110) surface. Model 1 describes the surface charge in terms of bulk-building blocks and point-charge transfers between such units dictated by the electron counting rule; model 2 is an attempt to take into account atomic relaxation and further charge redistribution among the bonds within the blocks (see text).

	(100)					(110)
	c-(4×4)	$(2\times4)\beta$	$(2\times4)2\beta$	$(4\times2)\zeta$	$(4\times2)2\beta$	
Model 1	0	0.49	0.17	−0.10	−0.17	0
Model 2	0	0.19	0.03	−0.26	−0.15	0
Ab initio	−0.01	0.45	0.01	−0.06	−0.25	0

reference value is zero for both the (100) c-(4×4) and the (110) surface, consistent with the almost identical *ab initio* values of the IP for these surfaces. A reduction of the IP, relative to the reference value, by -0.17 eV and -0.10 eV is predicted for the (100) $(4\times2)2\beta$ and ζ structures, respectively. This is also consistent with the trends found for these Ga-rich structures from first principles. Finally, for the As-rich (100) $(2\times4)2\beta$ and β reconstructions, variations of $+0.17$ eV and $+0.49$ eV are obtained from the model. The variation for the 2β structure is somewhat overestimated, but that of the β configuration agrees very well with the *ab initio* result. The ordering of the resulting IP values is also consistent with that of the *ab initio* calculations for all the structures.

The model could be improved by considering electronic charge transfers between bonds rather than between ions, and by including the effect of atomic relaxation. To model the electronic transfers between bonds, we consider electrons located at midbond. The charge transfers for the $(4\times2)\zeta$ structure are illustrated in Fig. 7(b). The effect of atomic relaxation is included within linear-response theory (LRT), by considering the dipole produced by displacing ions with effective longitudinal charges Z_L^* [see Fig. 7(c)] as obtained in *ab initio* calculations for the surface atoms.[43] The dipole induced by the electronic transfers between bonds is exactly zero in the case of the (100) c-(4×4) and (110) surfaces. The (100) c-(4×4) surface does not show significant atomic relaxation perpendicular to the surface, and the IP change for the (110) surface due to atomic relaxation is also negligible (20 meV). Model improvements, therefore, concern only the (100) (4×2) and (2×4) surfaces. For the latter surfaces, the two contributions are large in magnitude and opposite in sign. It is therefore important to include them simultaneously to obtain meaningful results. The two contributions are indeed related, since when the electronic charge is transferred between bonds rather than between ions, the center of gravity of the electronic and ionic charges of the atoms do not coincide any more, and the electrostatic forces produce ionic relaxations towards the center of gravity of the electric charge, producing a counter dipole that tends to cancel the electronic one.

The model predictions obtained including the above two effects are also reported in Table II (model 2). Although the order of magnitude of the predicted IP changes and the IP ordering are not modified by these contributions (except for the ζ structure), the results are somewhat worse than those of model 1. We believe this is due in large part to cancellation errors between the ionic and electronic contributions, which in the model are approximated using two different schemes.

The dipole-model approach based on the ECR (especially in its simpler form, i.e., model 1) provides a satisfactory general description of the IP trends with surface atomic geometry and highlights the dominant mechanisms behind the observed IP changes.

V. CONCLUSIONS

We have performed *ab initio* calculations for GaAs(110) and (100) surfaces to investigate the behavior of the IP with surface geometry. For the polar (100) surface, we have examined various structures to understand the role of surface reconstruction and stoichiometry. We considered the As-rich c-(4×4), $(2\times4)\beta$, and $(2\times4)2\beta$ reconstructions, as well as the Ga-rich $(4\times2)2\beta$ and $(4\times2)\zeta$ structures. These structures are the lowest-energy structures which have been proposed so far for those reconstructions.

Our *ab initio* results are consistent with available experimental data on the IP and its behavior with surface morphology. Comparing our results to experiments, we propose that the maximum observed IP value corresponds to an As-terminated $(2\times4)\beta$ structure and the minimum to the Ga-rich $(4\times2)2\beta$ configuration. We have also presented a model, based on bulk sp^3-like building blocks and on the ECR, which allows us to understand and predict the trends of the IP changes with surface atomic geometry. This model generalizes previous results[8] by allowing comparison between a wider class of surface atomic geometries, including surfaces with different crystallographic orientations and reconstructions with different structural units.

ACKNOWLEDGMENTS

One of us (C.S.) acknowledges support from the Swiss National Science Foundation under Grant No. 20-67083.01. Computations were performed at the CSCS in Manno.

[1] Hölz and F.K. Schulte, in *Solid Surface Physics*, edited by G. Höhler and E.A. Niekisch, Springer Tracts in Modern Physics, Vol. 85 (Springer-Verlag, Berlin, 1979).
[2] A.G. Milnes, *Semiconductor Devices and Integrated Electronics* (Van Nostrand Reinhold, New York, 1980).
[3] *Physics and Chemistry of Alkali Metal adsorption*, edited by H.P. Bonzel, A.M. Bradshaw, and G. Ertl, (Elsevier, Amsterdam, 1989).
[4] See e.g., W.E. Spicer, Appl. Phys. **12**, 115 (1977).
[5] H. Tsuda and T. Mizutani, Appl. Phys. Lett. **60**, 1570 (1992).
[6] N. Inoue, T. Higashino, K. Tanahashi, and Y. Kawamura, J. Cryst. Growth **227–228**, 123 (2001).
[7] T. Higashino, J. Osaka, K. Tanahashi, M. Kikuchi, Y. Kawamura, N. Inoue, and Y. Homma, J. Cryst. Growth **209**, 431 (2000).
[8] W. Chen, M. Dumas, D. Mao, and A. Kahn, J. Vac. Sci. Technol. B **10**, 1886 (1992).
[9] R. Duszak, C.J. Palmstrom, L.T. Florez, Y.-N. Yang, and J.H. Weaver, J. Vac. Sci. Technol. B **10**, 1891 (1992).
[10] J. Massies, P. Devoldere, and N.T. Linh, J. Vac. Sci. Technol. **16**, 1244 (1979).
[11] W. Ranke, Phys. Rev. B **27**, 7807 (1983).
[12] M.D. Paschley, Phys. Rev. B **40**, 10 481 (1989).
[13] L. Adamowicz and M. Zbroszczyk, Surf. Sci. **377-379**, 247 (1997).
[14] J-L.A. Alves, J. Hebenstreit, and M. Scheffler, Phys. Rev. B **44**, 6188 (1991).

[15] G-X. Qian, R.M. Martin, and D.J. Chadi, Phys. Rev. B **37**, 1303 (1988).
[16] W.G. Schmidt and F. Bechstedt, Phys. Rev. B **54**, 16 742 (1996).
[17] D.M. Ceperley and B.J. Alder, Phys. Rev. Lett. **45**, 566 (1980).
[18] N. Troullier and J.L. Martins, Phys. Rev. B **43**, 1993 (1991).
[19] L. Kleinman and D.M. Bylander, Phys. Rev. Lett. **48**, 1425 (1982).
[20] J.R. Chelikowsky, M. Schlüter, S.G. Louie, and M.L. Cohen, Solid State Commun. **17**, 1103 (1975).
[21] C. Sgiarovello, N. Binggeli, and A. Baldereschi, Phys. Rev. B **64**, 195305 (2001).
[22] C.J. Fall, N. Binggeli, and A. Baldereschi, J. Phys.: Condens. Matter **11**, 2689 (1999).
[23] C. Berthod, N. Binggeli, and A. Baldereschi, Europhys. Lett. **36**, 67 (1996).
[24] N. Binggeli, P. Ferrara, and A. Baldereschi, Phys. Rev. B **63**, 245306 (2001).
[25] C.J. Fall, N. Binggeli, and A. Baldereschi, Phys. Rev. B **66**, 075405 (2002).
[26] H.J. Monkhorst and J.D. Pack, Phys. Rev. B **13**, 5188 (1976).
[27] G. Harbeke, O. Madelung, and U. Rössler, in *Semiconductors: Physics of Group IV Elements and III-V Compounds*, edited by O. Madelung and Landolt-Börnstein, New Series, Group III, Vol. 17, Pt. a (Springer-Verlag, Berlin, 1982), p. 220.
[28] R.J. Needs, J.P. Charlesworth, and R.W. Godby, Europhys. Lett. **25**, 31 (1994).
[29] J. Bardi, N. Binggeli, and A. Baldereschi, Phys. Rev. B **59**, 8054 (1999).
[30] D.K. Bielgelsen, R.D. Bringans, J.E. Northrup, and L.E. Swartz, Phys. Rev. B **41**, 5701 (1990).
[31] D.J. Chadi, J. Vac. Sci. Technol. A **5**, 834 (1987).
[32] J.E. Northrup and S. Froyen, Phys. Rev. Lett. **71**, 2276 (1993); Phys. Rev. B **50**, 2015 (1994).
[33] S.-H. Lee, W. Moritz, and M. Scheffler, Phys. Rev. Lett. **85**, 3890 (2000).
[34] M. Tmar, A. Gabriel, C. Chatillon, and I. Ansara, J. Cryst. Growth **69**, 421 (1984).
[35] G.-X. Qian, R.M. Martin, and D.J. Chadi, Phys. Rev. Lett. **60**, 1962 (1988).
[36] T. Ohno, Phys. Rev. Lett. **70**, 631 (1993).
[37] K. Hirose, E. Foxman, T. Noguchi, and M. Uda, Phys. Rev. B **41**, 6076 (1990).
[38] G.M. Guichar, C.A. Sebenne, and G.A. Garry, Phys. Rev. Lett. **37**, 1158 (1976).
[39] J. van Laar, A. Huijser, and T.L. van Rooy, J. Vac. Sci. Technol. **14**, 894 (1977).
[40] T.-C. Chiang, J.A. Knapp, M. Aono, and D.E. Eastman, Phys. Rev. B **21**, 3513 (1980).
[41] R. Smoluchowski, Phys. Rev. **60**, 661 (1941).
[42] S. Baroni, R. Resta, A. Baldereschi, and M. Peressi, in *Spectroscopy of Semiconductor Microstructures*, Vol. 26 of *NATO Advanced Studies Institute Series B: Physics*, edited by G. Fasol, A. Fasolino, and P. Luigi (Plenum, New York, 1989), p. 251; M. Peressi, N. Binggeli, and A. Baldereschi, J. Phys. D **31**, 1273 (1998).
[43] A. Ruini, R. Resta, and S. Baroni, Phys. Rev. B **57**, 5742 (1998).